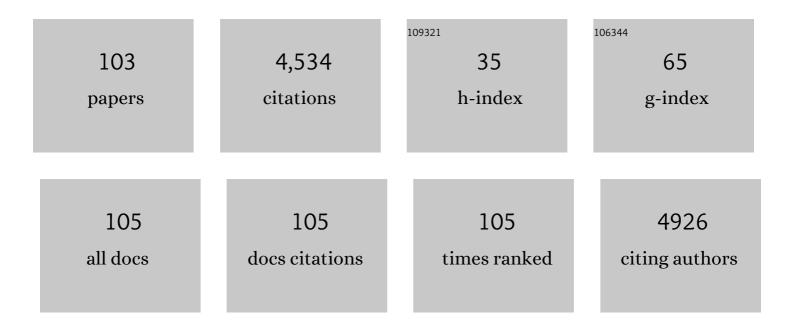


List of Publications by Year in descending order

Source: https://exaly.com/author-pdf/2216920/publications.pdf Version: 2024-02-01



#	Article	IF	CITATIONS
1	Intrinsic Electric Fields in Two-dimensional Materials Boost the Solar-to-Hydrogen Efficiency for Photocatalytic Water Splitting. Nano Letters, 2018, 18, 6312-6317.	9.1	391
2	Highly Efficient Photocatalytic Water Splitting over Edge-Modified Phosphorene Nanoribbons. Journal of the American Chemical Society, 2017, 139, 15429-15436.	13.7	244
3	A first-principles study of gas adsorption on germanene. Physical Chemistry Chemical Physics, 2014, 16, 22495-22498.	2.8	232
4	Silicene as a highly sensitive molecule sensor for NH3, NO and NO2. Physical Chemistry Chemical Physics, 2014, 16, 6957.	2.8	221
5	Defects in Phosphorene. Journal of Physical Chemistry C, 2015, 119, 20474-20480.	3.1	215
6	Edge-Modified Phosphorene Nanoflake Heterojunctions as Highly Efficient Solar Cells. Nano Letters, 2016, 16, 1675-1682.	9.1	176
7	Two-dimensional van der Waals heterojunctions for functional materials and devices. Journal of Materials Chemistry C, 2017, 5, 12289-12297.	5.5	151
8	Bidirectional photocurrent in p–n heterojunction nanowires. Nature Electronics, 2021, 4, 645-652.	26.0	129
9	Porous silicene as a hydrogen purification membrane. Physical Chemistry Chemical Physics, 2013, 15, 5753.	2.8	127
10	Tunable Schottky contacts in hybrid graphene–phosphorene nanocomposites. Journal of Materials Chemistry C, 2015, 3, 4756-4761.	5.5	116
11	Effects of interlayer coupling and electric fields on the electronic structures of graphene and MoS ₂ heterobilayers. Journal of Materials Chemistry C, 2016, 4, 1776-1781.	5.5	114
12	Large birefringence liquid crystal material in terahertz range. Optical Materials Express, 2012, 2, 1314.	3.0	104
13	Half-Metallicity in Organic Single Porous Sheets. Journal of the American Chemical Society, 2012, 134, 5718-5721.	13.7	101
14	Electronic and optical properties of graphene and graphitic ZnO nanocomposite structures. Journal of Chemical Physics, 2013, 138, 124706.	3.0	97
15	Helium separation via porous silicene based ultimate membrane. Nanoscale, 2013, 5, 9062.	5.6	96
16	Highly-efficient heterojunction solar cells based on two-dimensional tellurene and transition metal dichalcogenides. Journal of Materials Chemistry A, 2019, 7, 7430-7436.	10.3	90
17	First-principles study of two-dimensional van der Waals heterojunctions. Computational Materials Science, 2016, 112, 518-526.	3.0	88
18	Structural, electronic, and optical properties of hybrid silicene and graphene nanocomposite. Journal of Chemical Physics, 2013, 139, 154704.	3.0	84

#	Article	IF	CITATIONS
19	Semiconductor Alloy Nanoribbon Lateral Heterostructures for Highâ€Performance Photodetectors. Advanced Materials, 2014, 26, 2844-2849.	21.0	70
20	Metal-Free Boron Nitride Nanoribbon Catalysts for Electrochemical CO ₂ Reduction: Combining High Activity and Selectivity. ACS Applied Materials & Interfaces, 2019, 11, 906-915.	8.0	66
21	Systematic Synthesis of Tellurium Nanostructures and Their Optical Properties: From Nanoparticles to Nanorods, Nanowires, and Nanotubes. ChemNanoMat, 2016, 2, 167-170.	2.8	61
22	Hydrogenâ€Dopingâ€Induced Metalâ€Like Ultrahigh Freeâ€Carrier Concentration in Metalâ€Oxide Material for Giant and Tunable Plasmon Resonance. Advanced Materials, 2020, 32, e2004059.	21.0	57
23	DGDFT: A massively parallel method for large scale density functional theory calculations. Journal of Chemical Physics, 2015, 143, 124110.	3.0	55
24	A Machine Learning Protocol for Predicting Protein Infrared Spectra. Journal of the American Chemical Society, 2020, 142, 19071-19077.	13.7	55
25	Tunable Rashba spin splitting in Janus transition-metal dichalcogenide monolayers <i>via</i> charge doping. RSC Advances, 2020, 10, 6388-6394.	3.6	55
26	Thermionic Energy Conversion Based on Graphene van der Waals Heterostructures. Scientific Reports, 2017, 7, 46211.	3.3	53
27	Interpolative Separable Density Fitting Decomposition for Accelerating Hybrid Density Functional Calculations with Applications to Defects in Silicon. Journal of Chemical Theory and Computation, 2017, 13, 5420-5431.	5.3	53
28	Tuning the Charge Transfer Dynamics of the Nanostructured GaN Photoelectrodes for Efficient Photoelectrochemical Detection in the Ultraviolet Band. Advanced Functional Materials, 2021, 31, 2103007.	14.9	50
29	Doped phosphorene for hydrogen capture: A DFT study. Applied Surface Science, 2018, 433, 249-255.	6.1	48
30	Diamond as an inert substrate of graphene. Journal of Chemical Physics, 2013, 138, 054701.	3.0	46
31	Photogenerated-Carrier Separation and Transfer in Two-Dimensional Janus Transition Metal Dichalcogenides and Graphene van der Waals Sandwich Heterojunction Photovoltaic Cells. Journal of Physical Chemistry Letters, 2020, 11, 4070-4079.	4.6	44
32	Electronic structure and aromaticity of large-scale hexagonal graphene nanoflakes. Journal of Chemical Physics, 2014, 141, 214704.	3.0	40
33	Interpolative Separable Density Fitting through Centroidal Voronoi Tessellation with Applications to Hybrid Functional Electronic Structure Calculations. Journal of Chemical Theory and Computation, 2018, 14, 1311-1320.	5.3	39
34	Adaptively Compressed Exchange Operator for Large-Scale Hybrid Density Functional Calculations with Applications to the Adsorption of Water on Silicene. Journal of Chemical Theory and Computation, 2017, 13, 1188-1198.	5.3	38
35	Two-Dimensional Giant Tunable Rashba Semiconductors with Two-Atom-Thick Buckled Honeycomb Structure. Nano Letters, 2021, 21, 740-746.	9.1	38
36	Edge reconstruction in armchair phosphorene nanoribbons revealed by discontinuous Galerkin density functional theory. Physical Chemistry Chemical Physics, 2015, 17, 31397-31404.	2.8	37

#	Article	IF	CITATIONS
37	Machine Learning K-Means Clustering Algorithm for Interpolative Separable Density Fitting to Accelerate Hybrid Functional Calculations with Numerical Atomic Orbitals. Journal of Physical Chemistry A, 2020, 124, 10066-10074.	2.5	35
38	Derived equivalences and stable equivalences of Morita type, I. Nagoya Mathematical Journal, 2010, 200, 107-152.	0.8	33
39	<mml:math <br="" altimg="si1.gif" xmlns:mml="http://www.w3.org/1998/Math/MathML">overflow="scroll"><mml:mi mathvariant="script">D</mml:mi></mml:math> -split sequences and derived equivalences. Advances in Mathematics, 2011, 227, 292-318.	1.1	33
40	[Ti ₁₂ In ₆ O ₁₈ (OOCC ₆ H ₅) ₃₀]: a multifunctional hetero-polyoxotitanate nanocluster with high stability and visible photoactivity. Dalton Transactions, 2017, 46, 678-684.	3.3	31
41	Adaptive local basis set for Kohn–Sham density functional theory in a discontinuous Galerkin framework II: Force, vibration, and molecular dynamics calculations. Journal of Computational Physics, 2017, 335, 426-443.	3.8	29
42	Chebyshev polynomial filtered subspace iteration in the discontinuous Galerkin method for large-scale electronic structure calculations. Journal of Chemical Physics, 2016, 145, 154101.	3.0	28
43	High-Throughput Screening of Rattling-Induced Ultralow Lattice Thermal Conductivity in Semiconductors. Journal of the American Chemical Society, 2022, 144, 4448-4456.	13.7	26
44	Room-temperature magnetism and tunable energy gaps in edge-passivated zigzag graphene quantum dots. Npj 2D Materials and Applications, 2019, 3, .	7.9	25
45	Tunable Schottky and Ohmic contacts in graphene and tellurene van der Waals heterostructures. Physical Chemistry Chemical Physics, 2019, 21, 23611-23619.	2.8	24
46	Accelerating Excitation Energy Computation in Molecules and Solids within Linear-Response Time-Dependent Density Functional Theory via Interpolative Separable Density Fitting Decomposition. Journal of Chemical Theory and Computation, 2020, 16, 964-973.	5.3	23
47	Tunable Rashba Spin Splitting in Two-Dimensional Polar Perovskites. Journal of Physical Chemistry Letters, 2021, 12, 1932-1939.	4.6	22
48	Spin–Orbit Coupling in 2D Semiconductors: A Theoretical Perspective. Journal of Physical Chemistry Letters, 2021, 12, 12256-12268.	4.6	22
49	Water on silicene: A hydrogen bond-autocatalyzed physisorption–chemisorption–dissociation transition. Nano Research, 2017, 10, 2223-2233.	10.4	21
50	Projected Commutator DIIS Method for Accelerating Hybrid Functional Electronic Structure Calculations. Journal of Chemical Theory and Computation, 2017, 13, 5458-5467.	5.3	21
51	Designing Direct Z-Scheme Heterojunctions Enabled by Edge-Modified Phosphorene Nanoribbons for Photocatalytic Overall Water Splitting. Journal of Physical Chemistry Letters, 2022, 13, 1-11.	4.6	21
52	Stable Heteropolyoxotitanate Nanocluster for Full Solar Spectrum Photocatalytic Hydrogen Evolution. Journal of Physical Chemistry C, 2017, 121, 18326-18332.	3.1	20
53	A modified Schottky model for graphene-semiconductor (3D/2D) contact: A combined theoretical and experimental study. , 2016, , .		19
54	Interpolative Separable Density Fitting Decomposition for Accelerating Hartree–Fock Exchange Calculations within Numerical Atomic Orbitals. Journal of Physical Chemistry A, 2020, 124, 5664-5674.	2.5	18

#	Article	IF	CITATIONS
55	Surface and size effects on the charge state of NV center in nanodiamonds. Computational and Theoretical Chemistry, 2013, 1021, 49-53.	2.5	17
56	Pressure Sensors: A Flexible and Highly Pressure-Sensitive Graphene-Polyurethane Sponge Based on Fractured Microstructure Design (Adv. Mater. 46/2013). Advanced Materials, 2013, 25, 6691-6691.	21.0	17
57	Derived equivalences for \hat{I}_{1}^{1} -Auslander-Yoneda algebras. Transactions of the American Mathematical Society, 2013, 365, 5681-5711.	0.9	17
58	Low-Rank Approximations Accelerated Plane-Wave Hybrid Functional Calculations with k-Point Sampling. Journal of Chemical Theory and Computation, 2022, 18, 206-218.	5.3	17
59	Effects of line defects on the electronic properties of ZnO nanoribbons and sheets. Journal of Materials Chemistry C, 2017, 5, 3121-3129.	5.5	16
60	High performance computing of DGDFT for tens of thousands of atoms using millions of cores on Sunway TaihuLight. Science Bulletin, 2021, 66, 111-119.	9.0	16
61	Tunable n-type and p-type doping of two-dimensional layered PdSe ₂ <i>via</i> organic molecular adsorption. Physical Chemistry Chemical Physics, 2020, 22, 12973-12979.	2.8	15
62	Molecular Design to Enhance the Thermal Stability of a Photo Switchable Molecular Junction Based on Dimethyldihydropyrene and Cyclophanediene Isomerization. Journal of Physical Chemistry C, 2015, 119, 11468-11474.	3.1	14
63	Theoretical Design of a Two-Photon Fluorescent Probe for Nitric Oxide with Enhanced Emission Induced by Photoninduced Electron Transfer. Sensors, 2018, 18, 1324.	3.8	14
64	Influence of point defects on the electronic and topological properties of monolayer <mml:math xmlns:mml="http://www.w3.org/1998/Math/MathML"> <mml:msub> <mml:mi>WTe</mml:mi> <mml:mn>2Physical Review B, 2020, 102, .</mml:mn></mml:msub></mml:math 	:m a.2 <td>าl:เmsub></td>	าl:เ m sub>
65	Realizing Effective Cubic-Scaling Coulomb Hole Plus Screened Exchange Approximation in Periodic Systems via Interpolative Separable Density Fitting with a Plane-Wave Basis Set. Journal of Physical Chemistry A, 2021, 125, 7545-7557.	2.5	13
66	Quasi-Analytical Approach for Modeling of Surface-Enhanced Raman Scattering. Journal of Physical Chemistry C, 2015, 119, 28992-28998.	3.1	13
67	Visualizing subsurface defects in graphite by acoustic atomic force microscopy. Microscopy Research and Technique, 2017, 80, 66-74.	2.2	12
68	Identifying the structure of 4-chlorophenyl isocyanide adsorbed on Au(111) and Pt(111) surfaces by first-principles simulations of Raman spectra. Physical Chemistry Chemical Physics, 2017, 19, 32389-32397.	2.8	12
69	Accelerating Optical Absorption Spectra and Exciton Energy Computation via Interpolative Separable Density Fitting. Lecture Notes in Computer Science, 2018, , 604-617.	1.3	12
70	Control of highly anisotropic electrical conductance of tellurene by strain-engineering. Nanoscale, 2019, 11, 21775-21781.	5.6	11
71	Designing Two-Dimensional Versatile Room-Temperature Ferromagnets via Assembling Large-Scale Magnetic Quantum Dots. Nano Letters, 2021, 21, 9816-9823.	9.1	11
72	Bifacial Raman Enhancement on Monolayer Two-Dimensional Materials. Nano Letters, 2019, 19, 1124-1130.	9.1	10

#	Article	IF	CITATIONS
73	Two-level iterative solver for linear response time-dependent density functional theory with plane wave basis set. Journal of Chemical Physics, 2021, 154, 064101.	3.0	10
74	Derived equivalences from cohomological approximations and mutations of <i>î¦</i> -Yoneda algebras. Proceedings of the Royal Society of Edinburgh Section A: Mathematics, 2013, 143, 589-629.	1.2	9
75	KSSOLV-GPU: An efficient GPU-enabled MATLAB toolbox for solving the Kohn-Sham equations within density functional theory in plane-wave basis set. Chinese Journal of Chemical Physics, 2021, 34, 552-564.	1.3	9
76	KSSOLV 2.0: An efficient MATLAB toolbox for solving the Kohn-Sham equations with plane-wave basis set. Computer Physics Communications, 2022, 279, 108424.	7.5	9
77	Large birefringence smectic-A liquid crystals for high contrast bistable displays. Optical Materials Express, 2015, 5, 281.	3.0	8
78	Stable functors of derived equivalences and Gorenstein projective modules. Mathematische Nachrichten, 2017, 290, 1512-1530.	0.8	8
79	Gorenstein projective bimodules via monomorphism categories and filtration categories. Journal of Pure and Applied Algebra, 2019, 223, 1014-1039.	0.6	8
80	Highly efficient heterojunction solar cells enabled by edge-modified tellurene nanoribbons. Physical Chemistry Chemical Physics, 2020, 22, 28414-28422.	2.8	8
81	Derived equivalences and stable equivalences of Morita type, II. Revista Matematica Iberoamericana, 2018, 34, 59-110.	0.9	7
82	Monitoring Reaction Paths Using Vibrational Spectroscopies: The Case of the Dehydrogenation of Propane toward Propylene on Pd-Doped Cu(111) Surface. Molecules, 2018, 23, 126.	3.8	7
83	Editorial: Advances in Density Functional Theory and Beyond for Computational Chemistry. Frontiers in Chemistry, 2021, 9, 705762.	3.6	7
84	Nondecaying long range effect of surface decoration on the charge state of NV center in diamond. Journal of Chemical Physics, 2013, 138, 034702.	3.0	6
85	Energy Donor Effect on the Sensing Performance for a Series of FRET-Based Two-Photon Fluorescent Hg2+ Probes. Materials, 2017, 10, 108.	2.9	6
86	Derived equivalences and stable equivalences of Morita type, I. Nagoya Mathematical Journal, 2010, 200, 107-152.	0.8	6
87	Identifying Photocatalytic Active Sites of C ₂ H ₆ C–H Bond Activation on TiO ₂ via Combining First-Principles Ground-State and Excited-State Electronic Structure Calculations. Journal of Physical Chemistry Letters, 2022, 13, 6532-6540.	4.6	6
88	Bistable state in polymer stabilized blue phase liquid crystal. Optical Materials Express, 2012, 2, 1353.	3.0	5
89	Auslander-Reiten sequences and global dimensions. Mathematical Research Letters, 2006, 13, 885-895.	0.5	5
90	Hybrid MPI and OpenMP parallel implementation of large-scale linear-response time-dependent density functional theory with plane-wave basis set. Electronic Structure, 2021, 3, 024004.	2.8	4

#	Article	IF	CITATIONS
91	Tilting modules and representation dimensions. Journal of Algebra, 2010, 323, 738-748.	0.7	3
92	First-principles study of Pd single-atom catalysis to hydrogen desorption reactions on MgH2(110) surface. Chinese Journal of Chemical Physics, 2019, 32, 319-326.	1.3	3
93	Two-dimensional Ca4N2 as a one-dimensional electride [Ca4N2]2+·2eâ^' with ultrahigh conductance. Nanoscale, 2020, 12, 5578-5586.	5.6	3
94	On derived equivalences and homological dimensions. Journal Fur Die Reine Und Angewandte Mathematik, 2021, 2021, 59-85.	0.9	3
95	On Iterated Almost ν-Stable Derived Equivalences. Communications in Algebra, 2012, 40, 3920-3932.	0.6	2
96	Conjugation Length Effect on TPA-Based Optical Limiting Performance of a Series of Ladder-Type Chromophores. Materials, 2017, 10, 70.	2.9	2
97	The static parallel distribution algorithms for hybrid density-functional calculations in HONPAS package. International Journal of High Performance Computing Applications, 2020, 34, 159-168.	3.7	2
98	Parallel Implementation of Large-Scale Linear Scaling Density Functional Theory Calculations With Numerical Atomic Orbitals in HONPAS. Frontiers in Chemistry, 2020, 8, 589910.	3.6	2
99	Computational characterization of nanosystems. Chinese Journal of Chemical Physics, 2022, 35, 1-15.	1.3	2
100	Mixed magnetic edge states in graphene quantum dots. Multifunctional Materials, 2022, 5, 014001.	3.7	1
101	Feasible Catalytic Strategy for Writing Conductive Nanoribbons on a Single-Layer Graphene Fluoride. Journal of Physical Chemistry C, 2014, 118, 22643-22648.	3.1	0
102	Approximations, ghosts and derived equivalences. Proceedings of the Royal Society of Edinburgh Section A: Mathematics, 2020, 150, 813-840.	1.2	0
103	Dominant and global dimension of blocks of quantised Schur algebras. Mathematische Zeitschrift, 0, , 1.	0.9	0